

Velocity field in the region of the temperature minimum of the solar atmosphere. Preliminary results of a determination of the amplitude of the general velocity field

É. A. Gurtovenko, V. A. Sheminova, and R. J. Rutten

Main Astronomical Observatory, Ukrainian SSR Academy of Sciences, and Utrecht Astronomical Institute

(Submitted August 24, 1983)

Astron. Zh. 62, 124–131 (January–February 1985)

The amplitude of the general velocity field in the middle and upper layers of the photosphere were studied through an analysis of weak Fraunhofer lines observed in the near wings of the H and K Ca II lines. Recordings of the solar spectrum with a high spectral resolution, obtained with the Fourier spectrometer of the Kitt Peak Observatory for four positions on the solar disk, were used. The results confirm the principal well-known data on the amplitude of the velocity field in the middle layers of the photosphere derived earlier in other papers. It is also established that the radial and tangential components of this amplitude also continue to decrease with height in the upper photosphere, down to the heights of $\log \tau_5 \leq -3.0$ ($h \approx 450$ km) and $\log \tau_5 \leq -4.0$ ($h \approx 560$ km), respectively. These data indicate that the convective motions penetrate into the region of the temperature minimum and dominate there, at least down to the heights indicated above.

1. INTRODUCTION

The field of nonthermal velocities, or the so-called turbulence, is the most important characteristic of the structure of the solar and stellar photospheres. The "turbulence" determines the amount and character of non-radiative energy transfer from the convection zone into the upper layers of the photosphere and its fine structure. It influences the equivalent width and shape of the profiles of Fraunhofer lines, which are the most important source of information on the physical conditions in stellar photospheres.

The velocity field in the solar photosphere (at least within the framework of a homogeneous photospheric model and the concept of micro- and macroturbulence) has already been studied rather well.¹⁻⁵ However, in the upper photosphere and the region of the temperature minimum these data are meager, since the profiles of strong lines formed high up are insensitive to the velocity field. Moreover, the central intensities of strong lines can be significantly subject to the influence of a departure from LTE.

A tangential component of the amplitude of the general velocity field of ~ 2 km/sec was derived by Canfield⁶ from weak emission lines in the wings of the H and K Ca II lines. The same order of amplitude of the "turbulent" velocity in upper layers of the photosphere was obtained by Mount and Linsky⁷ from CN molecular lines. However, Porfir'eva⁸ obtained a value averaging close to 3.5 km/sec from weak lines of the same molecule. The radial component of the general velocity field in the upper photosphere was also determined by Ayres,⁹ using a series of weak absorption lines in the wings of the H and K Ca II lines. He obtained an amplitude $V^{\text{rad}} \approx 1.6$ km/sec not varying appreciably with depth. There are no more reliable data on the amplitude of the general velocity field in the region of the temperature minimum. The importance of the investigation of the velocity field in the transition region between the photosphere and chromosphere is also determined by other circumstances. In the region of the temperature minimum the condition of equilibrium formation

of Fraunhofer lines is violated, convective motions die out, and oscillating motions develop. The direct transfer of mechanical energy into the chromosphere and corona starts from this zone. Therefore, knowledge of the velocity field in this region can yield additional information about the connection between convection and the oscillations and about the mechanism of heating of the upper layers of the solar atmosphere. More specific questions are also altered. In particular, it is unclear why the amplitude of the general velocity field at this height is still so high. The velocities of convective motions should be close to zero there, while the velocities of oscillating motions do not reach 2 km/sec even in the chromosphere.

Preliminary results of a study of the amplitude of the general velocity field in the upper photosphere are obtained in the present paper.

2. OBSERVATIONAL MATERIAL AND METHOD OF INVESTIGATION

In the paper we used the solar spectrum in the region of the H and K Ca II lines for four positions on the disk: $\cos \theta = 1.0, 0.67, 0.45,$ and 0.20 . The solar spectrum, recorded on magnetic tape with an interval $\Delta \lambda \approx 2 \text{ m}\text{\AA}$, was obtained with the Fourier spectrometer of the Kitt Peak Observatory by R. Rutten. The Fourier spectrometer of the Kitt Peak Observatory provides observations of a practically ideal solar spectrum. A section of the spectrum near the $\lambda 3969.641$ Fe I and $\lambda 3969.755$ Cr I lines for $\cos \theta = 0.45$ is presented in Fig. 1 as an example.

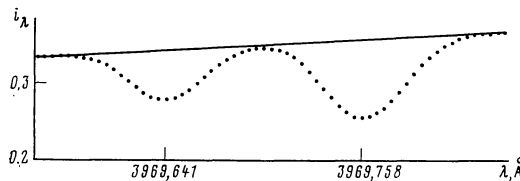


FIG. 1. Section of the wing of the H line (sloping straight line) containing the $\lambda 3969.641$ Fe I and $\lambda 3969.758$ Cr I lines based on observations with the Fourier spectrometer of the Kitt Peak Observatory, $\cos \theta = 0.45$; points plotted with an interval of $\sim 4 \text{ m}\text{\AA}$; i_λ is the intensity in relative units.

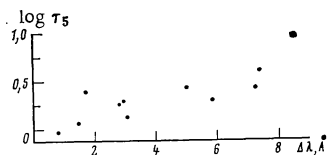


FIG. 2. Difference in depths of formation $\Delta \log \tau_5 = \log \tau_{5E} - \log \tau_{5D}$ (see Table II) as a function of the distance $\Delta \lambda$ from the center of the K line; $\cos \theta = 1$.

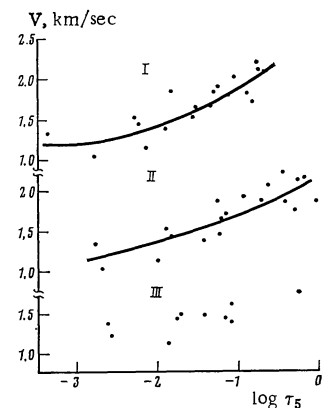


FIG. 3. Radial component ($\cos \theta = 1$) of the general velocity field: I) depths of line formation calculated from the depression contribution function; II) depths of line formation determined from the depth of formation of emission in the H and K line wings (Ayres's method); III) Ayres's results.⁹

In the present investigation we made a simplified analysis of the observational material by a method generally close to Ayres's method,⁹ viz.: 1) Only weak Fraunhofer lines were used (we chose lines with a central depth of no more than 30% of the intensity of the neighboring emission in the wings of the H and K Ca II lines); 2) we assumed that the depth of formation of the weak lines equals the depth of formation of the nearby emission in the H and K wings (Ayres's assumption). Thus, weak lines lying at different distances from the centers of the H and K lines yield information about the velocity field at the corresponding depths in the photosphere; 3) the profile of the lines under consideration is a Doppler profile with a half-width $\Delta \lambda_D = \frac{h}{1.66} = \frac{\lambda}{c} \sqrt{2RT/\mu + V^2}$, where h is the observed total half-width of the weak line while V is the "turbulent" velocity being sought. In contrast to Ayres, we did not use the complicated mechanism of partial coherent scattering to describe the H and K wings (at distances $\Delta \lambda > 0.5 \text{ \AA}$ from the centers of the lines). The line wings are sufficiently well described by the LTE condition and the Harvard-Smithsonian model photosphere with an excitation temperature close to the temperature of the Holweger-Muller model. Such an approximation does not cause significant errors at the medium depth of formation of emission in the H and K wings being calculated.

The results of such calculations made on the basis of the emission contribution function of Ref. 10 are presented in Table I. From the data of this table we constructed graphs, from which the depths of formation, for different distances $\Delta \lambda$ from the line center, were taken based on the quantity $\Delta \lambda$. This allowed us to find the temperature from the data of the photospheric model and to make an elementary determination of the amplitude of the general velocity field from the measured half-width h .

Ayres's assumption⁹ of equality of the depth of formation of weak Fraunhofer lines and the depths of formation of the nearby emission in the H and K wings is false. It may give results close to the truth only in so far as the depths of formation of emission and depression in very intense lines are close.¹⁰ Even in this case, however, weak absorption lines in the H and K wings are formed above the level of formation of the wings of these lines. Therefore, Ayres's depth scale defines the lower limit of the corresponding quantities. In this connection we made a more accurate (and fundamentally correct) calculation of the depths of formation of the same weak lines from the depression contribution function.¹⁰ Here we used the method of synthesis of blended Fraunhofer lines, i.e., in the expression $F_D = g \frac{\kappa_l}{\kappa_c} e^{-\tau_l}$ for the depression contribution function, the coefficient of selective absorption κ_l and the selective optical depth τ_l were determined by the sum of the absorption coefficients at the center of the corresponding weak line and the H (or K) line.

For the investigation in the H and K near wings we selected practically all the weak lines (in accordance with the above-indicated criterion) for which the half-widths could be determined sufficiently reliably. We excluded Co I lines owing to the possible broadening of their hyperfine structure. A list of the lines, their atomic parameters, and the central depths (with respect to the H or K wing) are presented in the first four columns of Table II. The wavelengths and excitation potentials are taken from the catalog of Moore et al.¹¹ Excitation potentials are not given in the catalog for four Fe I lines and the Nd II line. In the calculations of the depths of formation of the Fe I lines from the depression contribution function their excitation potentials were taken as 3.0 eV, which is close to the excitation potentials of all the other Fe I lines in our list. The depth of formation of the Nd II line was determined indirectly from graphs of the dependence of the difference $\Delta \log \tau_5 = \log \tau_{5E} - \log \tau_{5D}$ (columns 5-6, 8-9, 11-12, and 14-15 of Table II) on the distance $\Delta \lambda$ to the center of the K line. An example of such a dependence for $\cos \theta = 1$ is presented in Fig. 2.

TABLE I. Depths of Formation of Emission in the H and K Wings at Different Distances from the Line Center ($\Delta \lambda$) and from the Center of Solar Disk ($\cos \theta$)

$\Delta \lambda, \text{ \AA}$	K line				H line											
	$\cos \theta = 1.0$	$\cos \theta = 0.67$	$\cos \theta = 0.45$	$\cos \theta = 0.2$	$\cos \theta = 1.0$	$\cos \theta = 0.67$	$\cos \theta = 0.45$	$\cos \theta = 0.2$								
0.50	458	-3.20	492	-3.50	526	-3.75	601	-4.3	406	-2.85	437	-3.08	469	-3.30	538	-3.82
0.75	394	-2.77	426	-2.98	458	-3.22	526	-3.75	342	-2.40	374	-2.64	405	-2.84	469	-3.30
1.00	349	-2.45	381	-2.67	412	-2.90	477	-3.35	295	-2.07	328	-2.30	360	-2.52	423	-2.97
1.50	283	-1.97	316	-2.20	348	-2.44	413	-2.90	230	-1.57	262	-1.80	295	-2.08	361	-2.52
2.00	237	-1.64	260	-1.87	302	-2.10	368	-2.60	184	-1.28	217	-1.50	249	-1.74	316	-2.20
2.50	202	-1.40	234	-1.60	266	-1.85	333	-2.35	150	-1.05	183	-1.27	215	-1.48	281	-1.95
3.50	148	-1.03	182	-1.25	215	-1.48	280	-1.95	95	-0.70	132	-0.92	166	-1.15	232	-1.60
5.00	90	-0.65	128	-0.9	163	-1.14	228	-1.58	46	-0.35	81	-0.58	117	-0.82	185	-1.28

Notes. In each column the geometrical depth in km is given on the left and the optical depth on a logarithmic scale on the right.

TABLE II. Data on the Lines Used and Results Obtained. The Central Depth is Expressed in Units of the Intensity of the Wing of the H or K Line

Wave-length (Å)	Element	Excitation potential (eV)	Central depth	cos θ=1.0			cos θ=0.67			cos θ=0.45			cos θ=0.2		
				log τ _{5E}	log τ _{5D}	V	log τ _{5E}	log τ _{5D}	V	log τ _{5E}	log τ _{5D}	V	log τ _{5E}	log τ _{5D}	V
3926.326	Ti I	2.58	0.20	-0.23	-0.80	2.12	-0.50	-0.91	2.58	-0.75	-1.11	2.80	-1.10	-1.50	3.08
3926.639	Cr I	4.53	0.11	-0.30	-0.74	2.10	-0.55	-0.86	2.43	-0.80	-1.04	2.62	-1.20	-1.40	2.89
3927.107	Nd II	—	0.08	-0.35	-0.88	1.71	-0.58	-1.00	2.21	-0.85	-1.20	2.33	-1.45	-1.55	2.62
3930.663	Y II	0.41	0.09	-1.20	-1.40	1.69	-1.42	-1.59	2.23	-1.66	-1.82	2.31	-2.14	-2.27	2.53
3930.889	Fe I	2.45	0.16	-1.29	-1.58	1.43	-1.50	-1.77	2.06	-1.74	-1.98	2.14	-2.23	-2.42	2.29
3932.254	Fe I	—	0.11	-2.03	-2.18	1.14	-2.26	-2.38	1.80	-2.49	-2.60	1.88	-2.96	-3.03	2.17
3932.915	Fe I	—	0.14	-2.72	-2.80	1.03	-2.95	-3.00	1.99	-3.20	-3.21	1.94	Very weak		
3935.319	Fe I	2.84	0.31	-1.86	-2.27	1.42	-2.11	-2.46	1.94	-2.33	-2.67	1.88	-2.81	-3.09	2.03
3936.557	Fe I	—	0.18	-1.25	-1.57	1.65	-1.47	-1.75	2.15	-1.70	-1.97	2.32	-2.19	-2.40	2.29
3938.630	Fe I	—	0.12	-0.67	-1.10	2.03	-0.92	-1.19	2.17	-1.14	-1.39	2.38	-1.59	-1.80	2.29
3939.518	Sc II	0.31	0.08	-0.50	-0.83	2.20	-0.76	-1.05	2.53	-0.90	-1.22	2.66	-1.38	-1.62	2.81
3942.155	Ce II	0.0	0.29	-0.10	-0.96	1.84	-0.35	-1.00	2.45	-0.65	-1.16	2.45	-1.0	-1.55	2.71
3963.845	Fe I	2.42	0.15	-0.99	-1.31	1.91	-1.22	-1.53	2.15	-1.42	-1.74	2.59	-1.89	-2.17	2.49
3966.824	Fe I	3.30	0.24	-1.46	-1.97	1.39	-1.69	-1.74	2.03	-1.95	-2.36	2.11	-2.40	-2.78	2.19
3967.975	Fe I	3.24	0.19	-2.79	-3.40	1.33	-3.03	-3.53	1.75	-3.29	-3.74	1.58	-3.77	-4.06	2.07
3969.641	Fe I	3.25	0.27	-1.91	-2.29	1.50	-2.14	-2.52	1.86	-2.39	-2.75	1.84	-2.83	-3.14	2.29
3970.495	Ni I	3.65	0.27	-1.30	-1.87	1.86	-1.50	-2.02	2.15	-1.73	-2.24	2.30	-2.20	-2.64	2.25
3971.826	Fe I	2.76	0.27	-0.76	-1.35	1.86	-0.97	-1.53	2.28	-1.20	-1.75	2.27	-1.64	-2.16	2.31
3972.916	Fe I	3.57	0.32	-0.48	-1.18	1.82	-0.71	-1.36	2.44	-0.94	-1.57	2.61	-1.38	-1.99	2.74

The product of the content of the element times the oscillator strength for the weak lines was determined in the calculations by matching the observed and calculated residual intensity in the line. For the H and K Ca II lines the oscillator strengths, content of the element, and damping constant were taken from Ayres's data.¹²

3. DISCUSSION OF RESULTS

The results obtained — the depths of formation of the lines derived by two methods (log τ_{5E} and log τ_{5D}) and the corresponding "turbulent" velocities (V) — are presented in columns 5-16 of Table II. The data are represented graphically in Figs. 3 and 4. The difference in the above-indicated depths (due to the slow temperature variation in high layers of the photosphere) has practically no influence on the determined amplitude (V) of the general velocity field. Therefore, one value of this quantity is given in Table II.

We note the following clearly expressed features of the results obtained.

1. The data obtained through an estimate of the depth of line formation by the two methods differ insignificantly in general. The direct calculation of the depths from the depression contribution function yields a scale shifted into higher layers of the photosphere, with different amounts of shift depending on the distance from the center of the H and K lines (see, e.g., Fig. 2). This as well as other features of the difference log τ_{5E} - log τ_{5D} for a concrete line are fully explained by peculiarities of the depths of formation of emission and depression discussed in Ref. 10.

In the further discussion of the results we shall consider the more precise data obtained by calculating the depth of line formation from the depression contribution function.

2. The amplitude of the velocity field grows in the center-to-limb transition. The tangential component (cos θ = 0.2) is considerably larger than the radial component (cos θ = 1).

3. A clearly expressed decrease in the amplitude of the general velocity field with height is observed.

4. The expected cessation of the decline in the amplitude of the general velocity field at large heights (log τ₅ < -3.0) is not noted (or is noted unreliably).

Let us proceed to a more detailed discussion of the results. The features noted in points 1 and 2 are not unexpected and are fully consistent with the numerous data of investigations of the general velocity field obtained by other methods. Moreover, the amplitude of the general field practically coincides with the other principal results in the depth range where these results are obtained most reliably. At the depth log τ₅ = -1.5, e.g., for the radial component we have: V_{rad} = 1.6 km/sec (Ref. 1); V_{rad} = 1.7 km/sec (Ref. 2); V_{rad} = 1.75 km/sec (Ref. 3); V_{rad} = 1.7 km/sec (Ref. 5); V_{rad} = 1.7 km/sec in the present work. For the tangential component at the same depth we have 2.6, 2.6, 2.5, 2.7, and 2.8 km/sec, respectively.

Now we turn to the detailed features of the results obtained. The fact of a decrease in the "turbulent" velocity with heights is explained by the damping of convective

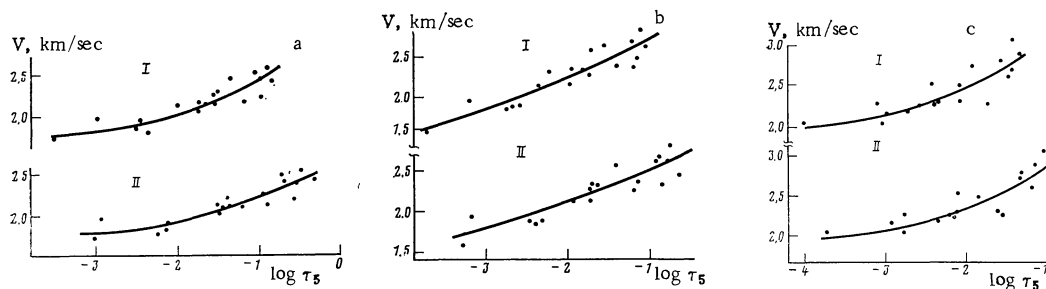


FIG. 4. Same results as in Fig. 3 I and II, respectively, for the positions cos θ = 0.67 (a), cos θ = 0.45 (b), and cos θ = 0.2 (c) on the solar disk.

TABLE III. Comparison of Optical Depths ($\log \tau_5$) and Amplitudes of the General Velocity Field (V) at the Center of the Disk Derived by Ayres (A) and in the Present Investigation of Gurtovenko, Sheminov, and Rutten (GShR)

$\lambda, \text{\AA}$	Element	$\log \tau_{5A}$	$\log \tau_{5GShR}$	V_A	V_{GShR}
3927.107	Nd II	-0.30	-0.35	1.79	1.71
3930.665	Y II	-1.15	-1.20	1.41	1.69
3930.881	Ti II	-1.22	-1.29	1.46	1.43
* 3932.017	Fe I	-1.78	-1.84	1.65	1.67
3932.250	Fe I	-1.90	-2.03	1.13	1.14
* 3932.635	Fe I	-2.20	-2.40	1.65	1.65
3932.923	Fe I	-2.60	-2.72	1.23	1.03
3935.314	Fe I	-1.78	-1.86	1.52	1.42
3936.547	Fe I	-1.14	-1.25	1.63	1.65
3966.819	Fe I	-1.45	-1.46	1.50	1.39
3967.972	Fe I	-2.65	-2.79	1.38	1.33
3969.635	Fe I	-1.78	-1.91	1.44	1.50
* 3969.751	Cr I	-1.70	-1.79	1.65	1.78

Note. Asterisks mark lines that we additionally analyzed in order to increase the total number of lines compared. The wavelengths of the lines are those given by Ayres.

motions, which evidently make the main contribution to the field of nonthermal motions in the photosphere. It is well known, however, that the turbulent velocity is higher in the chromosphere than in the photosphere. Its amplitude grows with height. Therefore, at certain heights one should observe a minimum in the amplitude of the general velocity field. We do not reliably observe such a minimum; it is clearly noted only for the radial component. We note that the character of the decrease is nearly linear, especially for $\cos \theta = 0.45$. The nonlinearity is displayed most clearly at the center of the disk and for $\cos \theta = 0.67$ and 0.20 , and has the same character. The decay of the radial component ($\cos \theta = 1$) slows abruptly at the depth $\log \tau_5 = -3.0$. Evidently, increases in the amplitude of the radial component can be explained at heights of $\log \tau_5 < -3.0$, i.e., from this height the vertically propagating sound waves or other processes responsible for the inhomogeneity of the lower chromosphere already make a significant contribution to the radial component of the general velocity field. The depth of the minimum in the amplitude of the tangential component is noted less reliably owing to the inadequacy of the observational material. One can only state that this minimum sets in at heights of $\log \tau_5 \leq -4.0$.

The indicated features of the behavior of the amplitude of the general velocity field in the upper photosphere undoubtedly reflect the nature of the photospheric field of nonthermal motions, the connection between convection and the oscillations, and also, possibly, the presence of a chaotic (turbulent) component in the field of nonthermal motions. Additional data on the velocity field at still greater heights, up to $\log \tau_5 = -(5.0-6.0)$, are required for a more well-founded discussion of this question. It is also proposed to obtain the data through a precise synthesis of a number of intense lines located very close to the cores of the H and K Ca II lines. For now, a single reliable conclusion can be drawn on the basis of the material obtained: convective motions extend high into the photosphere and dominate in the general velocity field in the radial direction to heights of $\log \tau_5 \leq -3.0$ ($h \approx 450$ km) and in the tangential direction to heights of $\log \tau_5 \leq -4.0$ ($h \approx 560$ km).

In conclusion, we turn to Ayres's results.⁹ In Fig. 3c we presented results taken from the data of Table I in his paper for lines common with the lines of our table. As is

seen, with allowance for the smaller number of lines used by Ayres, as well as for the dispersion of the points in the graphs, his results practically coincide with ours (Fig. 3b). For a more detailed comparison of the results, in Table III we present the optical depths and turbulent velocities derived by us and by Ayres for the lines common to his and our work. To use all of his data, at the center of the disk we made an additional analysis of the $\lambda\lambda$ 3932.017 Ti I, 3932.635 Fe I, and 3969.751 Cr I lines (Ayres's wavelengths), which were not included in our list (Table II) because of their high intensity.

As is seen, the results practically coincide. One can only note a small difference in the depth scale: on our scale the depths of line formation are somewhat lower on the average. A question arises: why did Ayres arrive at the incorrect conclusion that variation of the radial component of the velocity field with height is absent? In our opinion, this conclusion was furthered by the inclusion of the above-indicated three strong lines in the total relatively small number of lines used by the author. As a consequence of saturation, strong lines have larger half-widths and yield overstated values of the turbulent velocity. Further, on the basis of this conclusion Ayres draws a second false conclusion, that the $\lambda\lambda$ 3932.250, 3932.923, and 3967.972 Å iron lines (we note that these lines are formed the highest) are incorrectly identified in the catalog of Moore et al.,¹¹ since the "turbulent" velocity derived from them proves to be lower than that based on all the other lines. On this basis he "reidentifies" them, choosing a suitable atomic weight so as to reconcile their calculated and observed half-widths at the average turbulent velocity for the group of all the other lines.

Thus, Ayres's results agree well with the results of the present research and confirm all the features of the radial component of the general photospheric velocity field obtained earlier by other investigators.

4. CONCLUSIONS

1. The amplitudes of the general velocity field in the middle and upper photosphere agree well with the results of investigations made earlier by other reliable methods (Refs. 1-3, 5).

2. The decrease in the amplitude of the radial and